

Q1

Cite this: DOI: 10.1039/c3cy01051a

Q2

Selectivity in the catalytic hydrogenation of cinnamaldehyde promoted by Pt/SiO₂ as a function of metal nanoparticle size

Yujun Zhu and Francisco Zaera*

Received 13th December 2013,
Accepted 6th January 2014

DOI: 10.1039/c3cy01051a

www.rsc.org/catalysis

The structure sensitivity of the catalytic hydrogenation of cinnamaldehyde was studied by carrying out comparative studies with Pt/SiO₂ catalysts of various metal loadings, between 0.5 and 5.0 Pt wt%. Transmission electron microscopy (TEM) characterization was complemented with carbon monoxide adsorption experiments using infrared absorption spectroscopy and with kinetic studies under high (10 bar) pressures of H₂. Specific total turnover frequencies, normalized by the number of exposed Pt atoms, were found to correlate with both the average diameter of the metal nanoparticles and the average number of CO molecules adsorbed on flat terraces. It was concluded that cinnamaldehyde conversion is likely to take place on close-packed (111) planes. The selectivity between the hydrogenation of C=C versus C=O bonds, on the other hand, appears to be independent of either the particle size or the extent of the conversion, at least within the Pt particle size range explored in this study.

1. Introduction

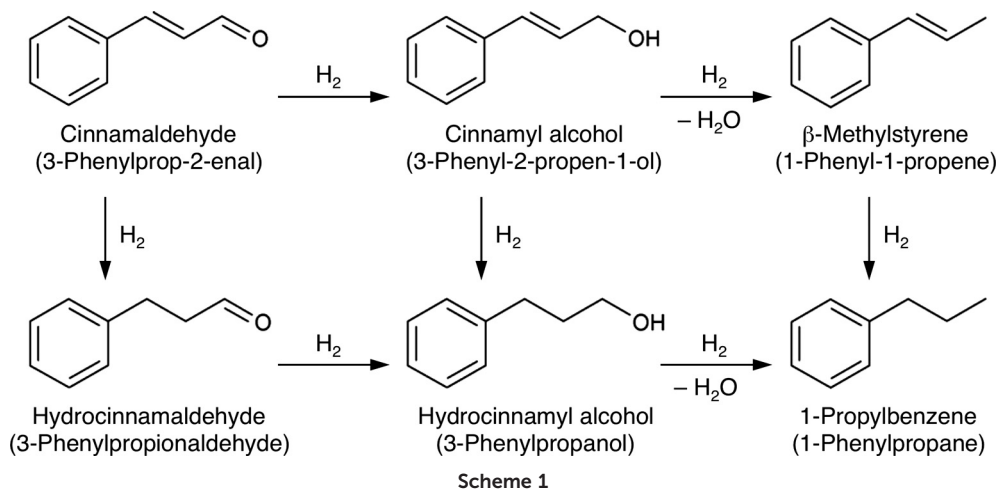
Selectivity has in recent years become a critical criterion for the design of catalytic processes.^{1,2} One way of tuning selectivity in such processes is by controlling the structure of the surfaces of heterogeneous catalysts.^{3–5} In a catalyst consisting of an active phase finely dispersed over a high-surface-area support, the active nanoparticles may be synthesized with specific sizes and/or shapes for this purpose.^{6–10} Such structure sensitivity is well known in demanding reactions such as ammonia synthesis,^{11,12} Fischer-Tropsch synthesis,¹³ and oil reforming.^{14,15} Mild reactions such as organic hydrogenations, by contrast, have traditionally been considered structure insensitive.¹⁶ However, new surface-science and catalytic evidence using well-defined catalysts has brought this conclusion into question.^{17–20} For instance, in a series of experiments in our laboratory, it was shown that the *cis-trans* isomerization of olefins is affected by the structure of the surface of the platinum catalysts used, with (111) planes favoring the formation of the less thermodynamically stable *cis* isomers.^{21–23}

The selective hydrogenation of C=O versus C=C bonds in unsaturated aldehydes is another good candidate for testing as a function of surface structure.^{24–26} The selective hydrogenation of the C=O bond is highly desirable, since it affords the production of unsaturated alcohols used in the production of flavorings, perfumes, and pharmaceuticals, but difficult because of their relative thermodynamic stability compared

to that of the C=C bonds (Scheme 1). Many studies have been published on the catalytic hydrogenation of unsaturated aldehydes, of cinnamaldehyde in particular, using transition metals in both the colloidal nanoparticle form^{27–29} and as heterogeneous catalysts,^{30–32} but those have reported quite different selectivities for the formation of unsaturated alcohol. Some recent reports on research using catalysts based on colloidal nanoparticles have also pointed to potential improvements in activity and selectivity as a function of nanoparticle size³³ or shape,^{34,35} but those trends have not proven to be universal, and other groups have reported no structure sensitivity for these reactions; research on this system continues to this day to try to settle these contradictions.^{36,37} It should be indicated that, with colloidal nanoparticles in particular, there is an issue with the effect that the surfactants used in their synthesis may exert on the performance of the catalyst.^{38–40} Therefore, it is important to test the size-dependence of this catalysis using more conventional catalysts.

In this study, we set out to investigate the structure sensitivity of the hydrogenation of unsaturated aldehydes on traditional metal catalysts. It was found that the hydrogenation of cinnamaldehyde on Pt-based catalysts is indeed dependent on the size of the metal nanoparticles. Correlations between particle sizes, CO adsorption data, and specific turnover frequencies point to an overall activity requiring sites on flat surfaces. Selectivity, on the other hand, appears to not depend in any significant way on particle size or the extent of conversion, at least within the particle size range studied here. These two conclusions, taken together, highlight the problem of studying structure sensitivity in catalysis by

Department of Chemistry, University of California, Riverside, CA 92521, USA.
E-mail: zaera@ucr.edu



correlating performance with particle size only instead of separating the effects of size *versus* surface structure. More details are provided below.

2. Experimental details

The platinum catalysts were prepared by a standard impregnation method. An appropriate weight of an 8 wt% H_2PtCl_6 solution in water (Sigma-Aldrich; 2.668, 5.363, 10.835, 16.420, 21.894 and 27.367 g for the 0.5, 1.0, 2.0, 3.0, 4.0, and 5.0 Pt wt% catalysts, respectively) was added to a slurry made out of 2.00 g of Aerosil 200 in deionized water, stirred at room temperature overnight and then dried slowly at about 343 K using a rotary evaporator. The resulting pale yellow fine powders were calcined in air at 673 K for 4 h to obtain the final gray catalysts.

Transmission electron microscopy (TEM) characterization of the resulting catalysts was carried out using a Tecnai T12 instrument capable of sub-nm resolution. CO adsorption was characterized by infrared (IR) absorption spectroscopy, as discussed elsewhere.^{41,42} The data were taken in transmission mode using a Bruker Tensor 27 Fourier-Transform IR (FTIR) spectrometer and a homemade quartz cell with NaCl windows capable of working at any temperature between 120 and 850 K and at any pressure between 0.01 and 1000 Torr.^{43,44} The catalysts were each pressed into a self-supporting 13 mm diameter disc and placed inside the central holder of the reactor. They were dried at 425 K for 1 h, either *in situ* under vacuum inside the transmittance IR cell or *ex situ* under air in a furnace, and pre-treated by following two alternating oxidizing and reducing cycles at 625 K, under 200 Torr of O_2 and 200 Torr of H_2 , respectively, for 60 min each, and one final 30 min reducing treatment. Each catalyst disk was studied individually by cooling it down to below 120 K and exposing it to 10 Torr of CO for 5 min, after which the cell was evacuated. Transmission IR spectra were taken at 10 K intervals while warming the sample until reaching a temperature of 373 K. The infrared spectra of the adsorbed CO were recorded at a resolution of 4 cm^{-1} using a

mercury–cadmium–telluride (MCT) detector, and referenced to background traces recorded under similar conditions before CO adsorption.

For the kinetic catalytic measurements, 0.100 g of the catalyst was calcined again at 573 K under O_2 for 1 h, cooled down to room temperature, reduced in H_2 at 623 K for 3 h, cooled back down again to room temperature, and transferred under an Ar atmosphere into a 300 mL high-pressure Parr reactor containing a mixture of the reactants, namely, 70 mL of isopropanol, about 0.41 g of phenylmethanol, and 0.800 g of cinnamaldehyde. The reactor was then pressurized with 10 bar of H_2 and stirred continuously during the course of the reaction, which was carried out at room temperature (300 K). Aliquots of the reaction mixture were taken periodically and analyzed by gas chromatography (HP50 Column $15\text{ m} \times 0.32\text{ mm} \times 0.25\text{ }\mu\text{m}$, FID detection). Identification of the products was achieved by comparing the retention times to those of reference compounds, and quantitative analysis of the mixtures was performed *via* calibration curves using phenylmethanol as an internal standard. All final data were obtained by subtracting the blank activity of the reactor, which was measured independently and amounted to a few percent of conversion over the entire length of time of the experiments.

3. Results

The catalysts were first characterized by TEM. Typical TEM images and size distributions are displayed for all six catalysts used in this study in Fig. 1. Average sizes ($\langle d \rangle$) and standard deviations are reported as well. In general, the size of the particles increased with metal loading, but the trend was not entirely monotonic; the 3.0 and 5.0 wt% Pt/ SiO_2 catalysts displayed average particle sizes below those expected on the basis of the numbers obtained with the other catalysts. Also, the size distributions were in general reasonably narrow, but deviated from Gaussian shape in some instances. Finally, nanoparticles of sizes below approximately 1.0 nm are difficult to detect in the TEM images, which

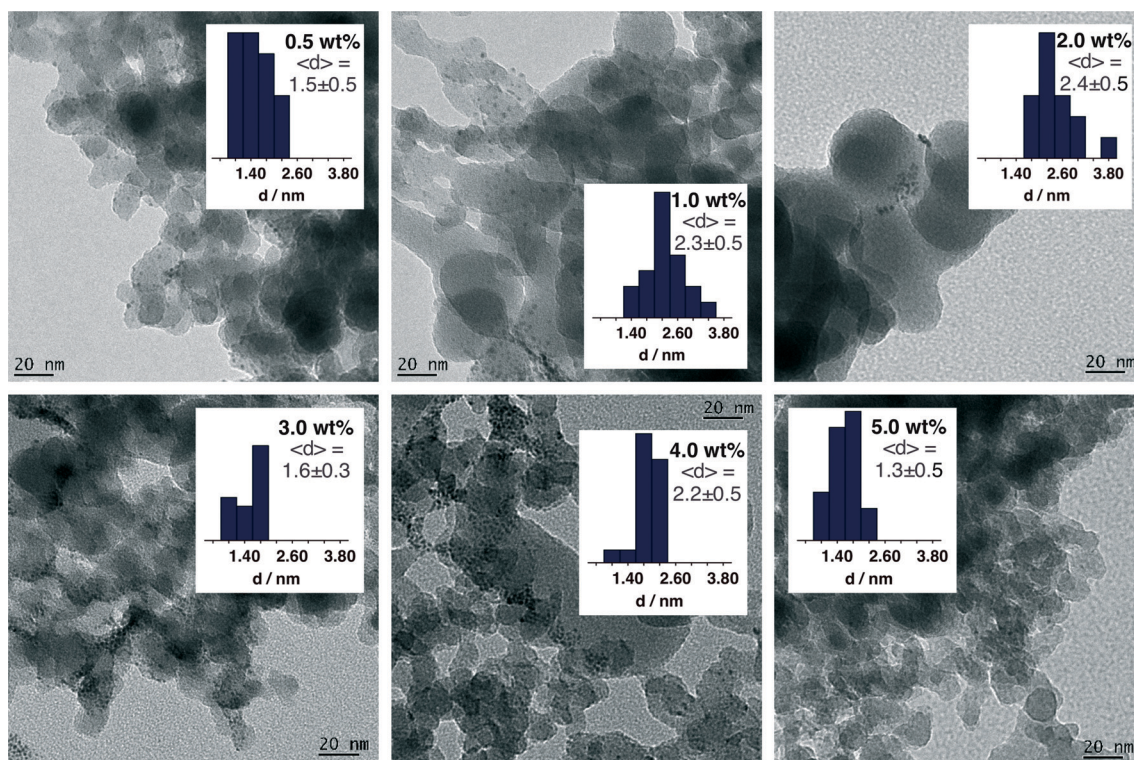


Fig. 1 Typical transmission electron microscopy (TEM) images for the Pt/SiO₂ catalysts employed in this study. Shown are images for all six metal loadings used, going from 0.5 to 5.0 Pt wt%. The insets provide the particle size distributions calculated from these images, as well as the corresponding average sizes and standard deviations.

means that the reported size averages may be overestimated in our report. This may be particularly important for the 0.5, 3.0, and 5.0 wt% samples.

CO IR titration experiments were carried out with all the Pt/SiO₂ catalysts in order to further characterize their metal surfaces. The left panel of Fig. 2 displays a typical sequence of spectra obtained after CO adsorption as a function of catalyst temperature (for the 2.0 wt% Pt/SiO₂) as the sample is warmed up from 123 to 373 K, while the right panel provides a summary of the evolution of the intensities of the different peaks detected for the C–O stretching mode. Several distinct features are seen in the IR spectra, at approximately 1630, 1870, 2100, 2160, and 2342 cm⁻¹. From these, the latter can be associated with the small amount of CO₂ that forms at low temperatures upon the reaction of CO with labile oxygen surface atoms, with O possibly left on the Pt surface after the oxidation–reduction pretreatment cycles. The peak at 1630 cm⁻¹ is likely to be due to CO adsorbed on interfacial Pt–SiO₂ sites, a temporary process seen as an intermediate step during the desorption of CO from the Pt surface; similar peaks have been observed in our laboratory with other types of supported catalysts.^{45,46}

The three remaining peaks are associated with CO adsorption on Pt. Indeed, the peak at ~2100 cm⁻¹, the main feature in most of our IR spectra, is well known to correspond to binding of carbon monoxide to atop sites of low Miller index terraces, most likely (111) planes.^{47,48} The exact position of the peak varies with temperature, in particular in between

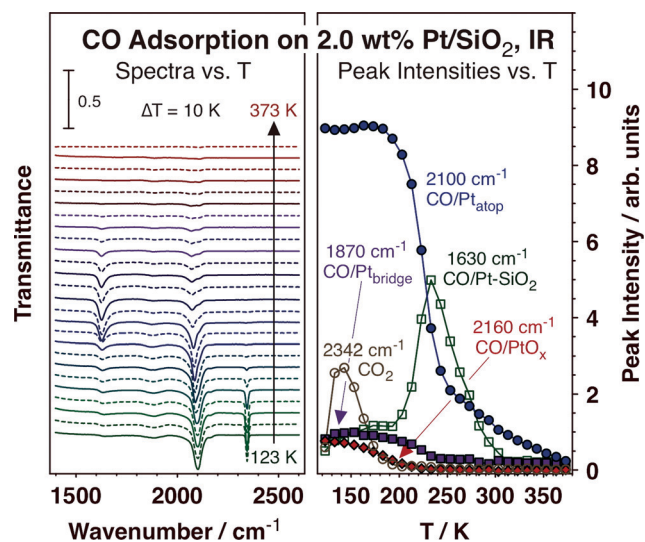


Fig. 2 Left: transmission infrared (IR) absorption spectra in the C–O stretching region obtained from the 2.0 wt% Pt/SiO₂ catalyst saturated with carbon monoxide at 120 K as a function of surface temperature, in the range 123 to 373 K (in 10 K intervals). Five main peaks can be identified from the data, at 1630 (CO on Pt–SiO₂ interfaces), 1870 (CO on bridged Pt sites), 2100 (CO on atop Pt sites), 2160 (CO on partially oxidized Pt), and 2342 (CO₂) cm⁻¹. Right: evolution of the peak intensities of the five IR peaks identified on the right as a function of surface temperature. The traces can be used to estimate the desorption temperature of each species.

approximately 150 (2100 cm⁻¹) and 200 K (2080 cm⁻¹), because of the changes in CO surface coverage upon CO

desorption.^{47,49} The maximum desorption rate for this species is seen at about 225 K. A second, weaker and broader feature is seen at approximately 1870 cm^{-1} , a frequency typical of CO adsorption on bridges or other high-coordination sites.⁴⁷ The intensity of this band is weaker, at least in part because of its intrinsically smaller absorption cross section, and desorption from this state occurs at slightly lower temperatures, at approximately 220 K. Importantly, the clear detection of this adsorption geometry attests to the presence of relatively wide terraces within the Pt nanoparticles. Finally, the small feature at 2160 cm^{-1} , seen mostly in the high-metal-loading catalysts, is due to adsorption on partially oxidized Pt,^{47,50,51} probably on atoms next to the interface with the support. The maximum desorption rate from those sites is seen at ~ 210 K.

The trends observed in the CO adsorption IR data as a function of Pt loading are summarized in Fig. 3. Typical spectra obtained at an adsorption temperature of 153 K are shown on the left panel, and the corresponding peak intensities measured for the three Pt-CO species collected are shown in the right panel. It can be observed that the number of Pt atop sites increases roughly linearly with metal loading, except for the last point, for the 5.0 Pt wt%, where the observed adsorption is less than the expected. Atop sites are presumably available in particles of any size, the reason for the linear signal increase with loading, but in this case the data seem to suggest that there is also a monotonic increase in the area of (111) terraces. On the other hand, a less pronounced variation in peak intensity is observed for the bridge-CO state, signifying that its population depends not only on metal loading but also on average particle

size. This is also noticeable, albeit to a lesser extent, in the behavior of the 2160 cm^{-1} peak, which reflects the evolution of the Pt-SiO₂ interfacial states.

Fig. 4 displays a typical kinetic run obtained for the conversion of cinnamaldehyde using our Pt/SiO₂ catalysts, the one with 1 Pt wt% loading in this case. Many products were detected, including those from selective hydrogenation of a single unsaturated bond (3-phenylpropionaldehyde, or hydrocinnamaldehyde, from hydrogenation of the C=C bond, and 3-phenyl-2-propen-1-ol, or cinnamyl alcohol, from hydrogenation of the C=O bond), from hydrogenation of both unsaturations in the side chain (3-phenylpropanol, or hydrocinnamyl alcohol) and from additional dehydration steps (1-phenyl-1-propene, or β -methylstyrene, and 1-propylbenzene, or 1-phenylpropane). The constant rate of formation of most of these products in the initial stages of the conversion is manifested by the linear nature of their accumulation curves, although there is an early offset in the production of 3-phenylpropionaldehyde, as also reported previously with Ru catalysts.⁵² Moreover, the primary nature of the production of the singly hydrogenated molecules and the secondary formation of the others is clearly seen by the change in kinetics around 5500 s, at which point the accumulated 3-phenylpropionaldehyde and 3-phenyl-2-propen-1-ol start to be consumed and the concentrations of the other products increase significantly.

More details of the kinetics of this reaction in terms of selectivity are provided in Fig. 5, which shows the evolution of the percentage composition of the product mixture as a function of conversion for both primary (left panel) and

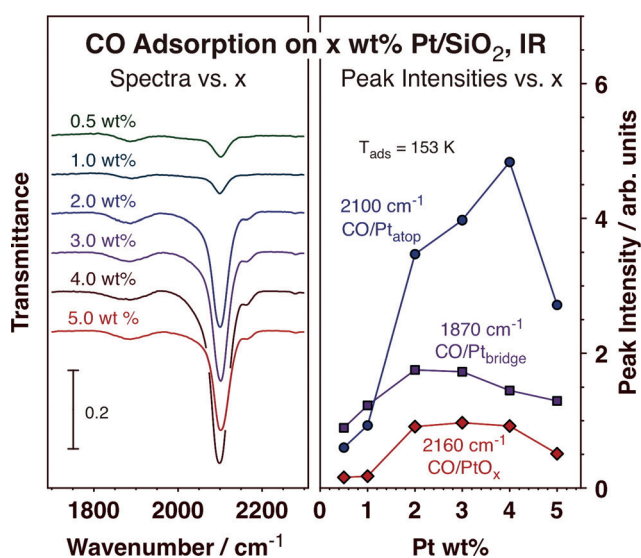


Fig. 3 Left: CO IR spectra from Pt/SiO₂ catalysts saturated with carbon monoxide at 153 K as a function of metal loading. Right: corresponding peak intensities. The focus in this figure is on the CO species adsorbed on platinum. The peak intensities correlate reasonably well with metal loading, but the dependence is weaker for the bridged CO species. The 2100 cm^{-1} peak provides a reasonable estimate of the area of the (111) planes in the Pt nanoparticles.

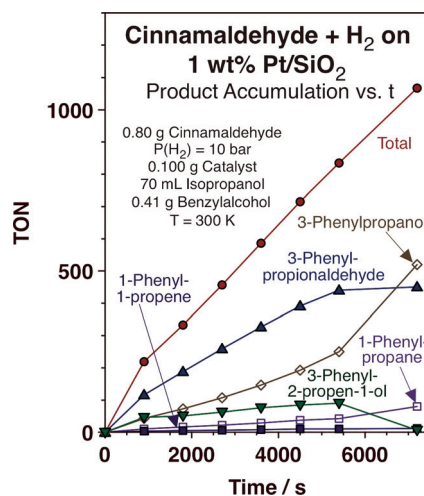


Fig. 4 Kinetic data for the catalytic hydrogenation of cinnamaldehyde promoted by the 1.0 wt% Pt/SiO₂ catalyst, in the form of the accumulation of the products versus reaction time. The reaction was carried out at room temperature (300 K) and under 10 bar of H₂. Traces are shown for the growth of the concentrations of both primary (3-phenylpropionaldehyde and 3-phenyl-2-propen-1-ol) and secondary (3-phenylpropanol, 1-phenylpropane, and 1-phenyl-1-propene) products. Approximate linear rates are seen for all species until about 5500 s, after which the accumulated primary products start to be converted to secondary products.

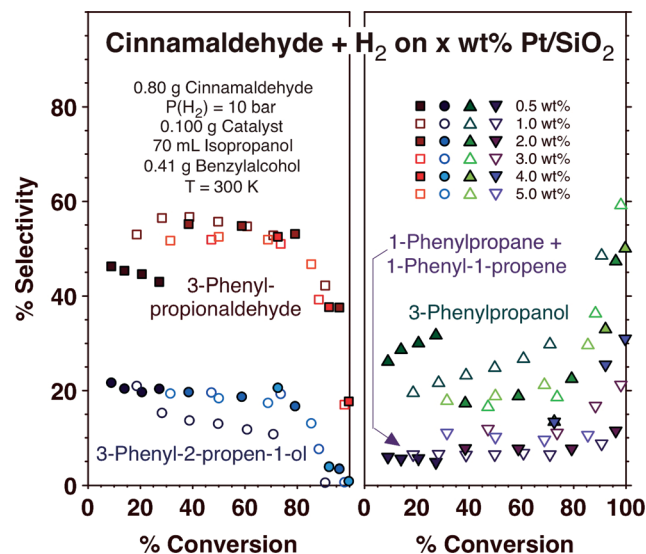


Fig. 5 Selectivity for the formation of both primary (3-phenylpropionaldehyde and 3-phenyl-2-propen-1-ol, left panel) and secondary (3-phenylpropanol and 1-phenylpropane plus 1-phenyl-1-propene, right) products as a function of total cinnamaldehyde conversion for reactions carried out with all Pt/SiO₂ catalysts, with Pt loadings going from 0.5 to 5.0 Pt wt%. In general, the primary selectivity between the hydrogenation of the C=C versus C=O bond is independent of both the metal loading and the extent of conversion.

secondary (right) products, obtained with all the six catalysts used in this study. In general, it can be seen that the selectivities for the production of the primary products are approximately constant as a function of conversion (below ~80%) and also independent of the metal loading used in the catalyst. A couple of exceptions to this conclusion are seen, however. First, the selectivity for these two products decreases drastically after 80% conversion because of their subsequent conversion to secondary products. Second, the selectivity for 3-phenyl-2-propen-1-ol does seem to decrease with conversion in the case of the 1.0 wt% Pt/SiO₂ catalyst. This is accompanied by a corresponding increase in 3-phenylpropanol formation, suggesting that the rate of C=O hydrogenation is still constant with conversion but that the subsequent hydrogenation of the C=C bond of the primary product (3-phenyl-2-propen-1-ol) may be relatively fast in some cases. Third, the selectivity for 3-phenylpropionaldehyde is lower on the small metal particles of the 0.5 wt% Pt/SiO₂ catalyst, although, again, this is compensated by the additional 3-phenylpropanol made in that case. Overall, it may be concluded from our kinetic data that the selectivity for the initial formation of 3-phenyl-2-propen-1-ol versus 3-phenylpropionaldehyde is independent of the metal loading or the extent of conversion.

A summary of the key kinetic information extracted from our studies is provided in Fig. 6. The right panel reports the initial selectivity measured with all catalysts. It corroborates the main conclusion from the previous paragraph, namely, that the selectivity between the hydrogenation of the C=C versus C=O bonds is not affected by the metal loading (the 0.5 Pt wt% being the exception, as discussed above),

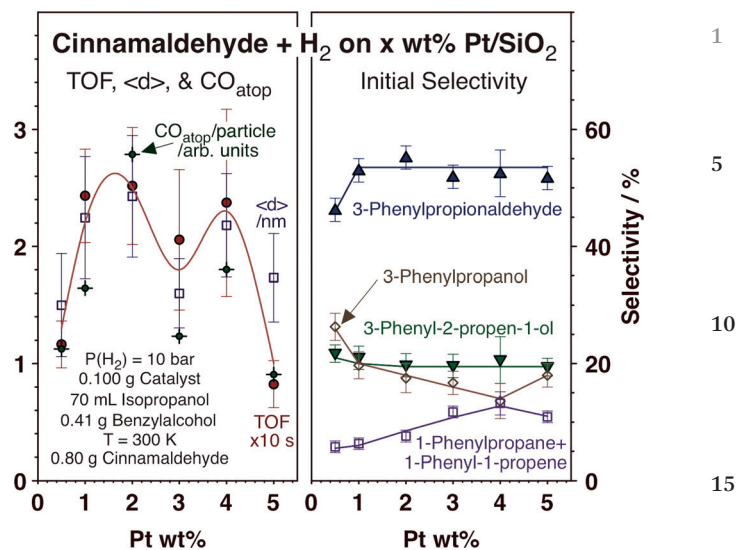


Fig. 6 Left: initial turnover frequencies (TOF, in cinnamaldehyde molecules converted per platinum atom per second), average Pt nanoparticle diameter (from the TEM images, in nm), and average number of CO molecules adsorbed on Pt atop sites (from the infrared absorption spectra, normalized by Pt wt% $\times \langle d \rangle^3$, in arbitrary units) as a function of metal loading. All three parameters show similar trends. Right: initial selectivities for both primary and secondary products as a function of metal loading. The primary selectivity shows virtually no dependence on Pt wt%, but decomposition of the fully hydrogenated 3-phenylpropanol and dehydration steps appear to be favored by the larger particles.

which is to say that it does not depend on particle size, at least in the ~1.5–2.5 nm range of our samples. There is, on the other hand, an increased preference for the decomposition of the fully hydrogenated 3-phenylpropanol and for the formation of dehydrated products, 1-phenylpropane and 1-phenyl-1-propene, on larger platinum particles. The latter of these two final products is the minor product in this case, possibly because once formed it can be easily hydrogenated to the former.

The data shown in the left panel of Fig. 6 can be used to extract correlations between the nature of the catalysts and their reactivity. Three parameters are reported there: (1) the total turnover frequency (TOF) for the conversion of cinnamaldehyde, expressed in terms of molecules decomposed per platinum atom per second; (2) the average Pt nanoparticle diameter ($\langle d \rangle$), extracted from the TEM images (Fig. 1); and (3) the average number of CO molecules adsorbed per particle (in arbitrary units), estimated from the atop CO IR signals in Fig. 3, normalized by the number of particles in the catalyst (which is proportional to the Pt wt% times the average particle size to the third power). It can be seen that all three parameters follow similar trends as a function of metal loading, suggesting that the conversion rate depends on the size of the particles. This is better illustrated by the plot in Fig. 7, where the TOF has been corrected by the fraction of platinum atoms exposed on the surface ($\#Pt_{\text{surface}}/\text{total } \#Pt$ for a given $\langle d \rangle$) and plotted versus the average particle size (instead of metal loading). An approximately linear

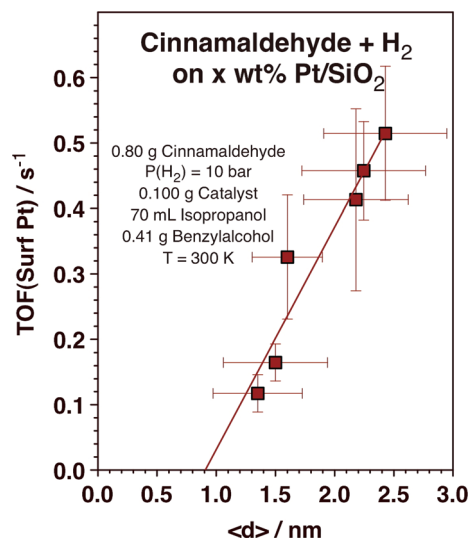


Fig. 7 Turnover frequencies normalized by the number of Pt surface atoms (TOF (surf Pt), estimated by using the average particle sizes $\langle d \rangle$ from the TEM images) as a function of $\langle d \rangle$. An approximately linear dependence is observed, suggesting the requirement of flat surfaces for the conversion of cinnamaldehyde. No conversion at all is estimated with particles smaller than $\langle d \rangle \leq 0.9$ nm.

dependence is seen in the graph, with an intercept predicting a total loss of activity for Pt particles smaller than ~ 0.9 nm. This suggests the need for Pt nanoparticles large enough to expose flat terraces, most likely (111) planes, in order to promote the cinnamaldehyde reaction. The CO IR data are consistent with this interpretation.

4. Discussion

Much work has been published already on the catalytic performance of transition metal catalysts for the hydrogenation of unsaturated aldehydes.^{24–26,30–32} One of the main interests has been to identify the conditions needed to improve the selectivity for the production of the unsaturated alcohol, and many articles have reported high selectivities for that reaction.^{30,32,53} It has also been suggested that the structure of the metal nanoparticles used as catalysts may contribute to the definition of this selectivity.^{30,33,34} However, a number of additional factors play a role in defining such selectivities, including the nature of the support,^{32,53} the catalyst pretreatment,^{53,54} the solvent,³⁷ and the addition of acidic promoters³³ and/or other metals,^{31,55} and those effects have not always been fully isolated in order to independently test the role of the structure of the catalyst. In addition, some of the past studies that have emphasized the role of the metal nanoparticle structure have been based on results obtained by using one or very few catalysts, and have therefore not provided good reference samples to contrast the effect of the different structural factors probed on catalytic activity and selectivity.³⁵

Here we focus on the effect of particle size on catalytic performance, and used simple Pt/SiO₂ catalysts to eliminate

most of the secondary effects mentioned above. Some of our observations are consistent with those of many other reports. In particular, we see an increase in overall catalytic activity with increase in Pt nanoparticle size. However, one of the main conclusions from our work is that there seem to be no significant differences in reaction selectivity associated with changes in the average diameter of those nanoparticles. The selectivity is also independent of the extent of conversion, except perhaps for an initial selective production of the hydrogenated aldehyde; some of those molecules may then remain adsorbed, modifying the subsequent reaction selectivity.⁵² It should be indicated that a few of the early reports on these systems relied on catalysts with wide ranges of particle sizes, in some cases between 1 and 15 nm;³⁰ this may be the reason for the apparent variations in activity and selectivity observed. Admittedly, in our study the particle size range used was relatively narrow, between approximately 1.5 and 2.5 nm in diameter, but this is the size range where the ratio of terrace to low-coordination surface sites varies in the most dramatic way; the surfaces of larger particles (used in many past studies) are usually dominated by terrace sites.

In addition, the increase in activity seen here as a function of nanoparticle size was directly associated with an increase in the fraction of metal atoms exposed as flat, possibly (111), planes. This conclusion is suggested by the dependence of the specific surface-normalized TOF values on particle size, and corroborated by the trends seen in the CO IR titration experiments. A past report using Ru catalysts claimed no effect of size on specific TOF,⁵² but the metal particles used in that case were quite large (3–20 nm), and large fractions of flat surfaces are likely there. A more recent study does show an increase in TOF with particle size, like in our case, even if the authors did not highlight that aspect of their results.³³

The two main conclusions of our work, namely, that primary selectivity does not depend on the structure of the catalyst or the extent of the reaction and that total activity is associated only with flat terraces, have not, to the best of our knowledge, been contrasted directly in the past, and point to the limitation of reaching conclusions regarding structure sensitivity in catalysis based solely on the dependence of catalytic performance on particle size. It is important to keep in mind that surface structure and total surface area both change with size but may exert different effects on such catalysis. Our conclusions also suggest that the conversion of cinnamaldehyde on Pt-based catalysts is limited by an initial step, possibly its adsorption, and that the adsorption geometry is fixed on those planes and determines the relative ratio of C=C *versus* C=O hydrogenation steps. Basic studies on this surface chemistry are sparse, but do in general support our hypothesis. The characterization of the adsorption of acrolein and crotonaldehyde on Pt(111) single-crystal surfaces carried out in our laboratory points to steric effects redirecting the potential flat adsorption of acrolein toward a preference for bonding through the C=C bond in more substituted unsaturated aldehydes.^{56,57} Similar steric effects on adsorption geometry have been predicted by DFT

calculations, although the structural details provided in that work follow the reverse trend, namely, a change from preferential C=C bonding in acrolein to flatter adsorption with increasing substitution.⁵⁸ Further calculations have also suggested a preference for C=O hydrogenation, but a selectivity affected by competitive desorption of the primary products (the unsaturated alcohol *versus* the hydrogenated aldehyde).^{36,59,60} The preferential initial formation of the hydrogenated aldehyde, before the selectivity sets to a constant value, and the competition seen in some cases between single and multiple hydrogenation steps (Fig. 5) provide some support for this conclusion.

5. Conclusions

The hydrogenation of cinnamaldehyde with Pt/SiO₂ catalysts under high pressures of hydrogen was studied as a function of the metal loading of the catalyst. Two main conclusions were reached from these studies: (1) the overall rate of reaction depends on the availability of low-Miller-index terraces, and (2) the primary hydrogenation selectivity does not depend on particle size, at least within the 1.5–2.5 nm particle size range. The data in this report are consistent with some previous publications (but also contrary to others), and with information from studies on model systems and quantum mechanics calculations. They point to the potentially different effects that surface structure and total surface area can exert on catalytic activity and selectivity.

Acknowledgements

Funding for this work was provided by a grant from the U. S. National Science Foundation.

References

- 1 F. Zaera, *J. Phys. Chem. B*, 2002, **106**, 4043.
- 2 G. A. Somorjai and J. Y. Park, *Angew. Chem., Int. Ed.*, 2008, **47**, 9212.
- 3 G. A. Somorjai, H. Frei and J. Y. Park, *J. Am. Chem. Soc.*, 2009, **131**, 16589.
- 4 F. Zaera, *J. Phys. Chem. Lett.*, 2010, **1**, 621.
- 5 F. Zaera, *ChemSusChem*, 2013, **6**, 1797.
- 6 I. Lee, M. A. Albiter, Q. Zhang, J. Ge, Y. Yin and F. Zaera, *Phys. Chem. Chem. Phys.*, 2011, **13**, 2449.
- 7 K. An and G. A. Somorjai, *ChemCatChem*, 2012, **4**, 1512.
- 8 K. Zhou and Y. Li, *Angew. Chem., Int. Ed.*, 2012, **51**, 602.
- 9 H. Lee, C. Kim, S. Yang, J. Han and J. Kim, *Catal. Surv. Asia*, 2012, **16**, 14.
- 10 F. Zaera, *Catal. Lett.*, 2012, **142**, 501.
- 11 N. D. Spencer, R. C. Schoonmaker and G. A. Somorjai, *J. Catal.*, 1982, **74**, 129.
- 12 A. Hellman, E. J. Baerends, M. Biczysko, T. Bligaard, C. H. Christensen, D. C. Clary, S. Dahl, R. van Harrevelt, K. Honkala, H. Jonsson, G. J. Kroes, M. Luppi, U. Manthe, J. K. Nørskov, R. A. Olsen, J. Rossmeisl, E. Skulason,

- 13 C. S. Tautermann, A. J. C. Varandas and J. K. Vincent, *J. Phys. Chem. B*, 2006, **110**, 17719.
- 14 R. A. van Santen, M. M. Ghouri, S. Shetty and E. M. H. Hensen, *Catal. Sci. Technol.*, 2011, **1**, 891.
- 15 B. C. Gates, J. R. Katzer and G. C. A. Schuit, *Chemistry of Catalytic Processes*, McGraw-Hill, New York, 1979.
- 16 J. H. Sinfelt, in *Catalysis - Science and Technology*, ed. J. R. Anderson and M. Boudart, Springer-Verlag, Berlin, 1981, vol. 1, pp. 257–300.
- 17 G. C. Bond, *Metal-Catalysed Reactions of Hydrocarbons*, Springer, New York, 2005.
- 18 R. Rioux, B. Hsu, M. Grass, H. Song and G. Somorjai, *Catal. Lett.*, 2008, **126**, 10.
- 19 F. Zaera, *Acc. Chem. Res.*, 2009, **42**, 1152.
- 20 N. R. Shiju and V. V. Gulianti, *Appl. Catal., A*, 2009, **356**, 1.
- 21 F. Zaera, *Phys. Chem. Chem. Phys.*, 2013, **15**, 11988.
- 22 I. Lee, F. Delbecq, R. Morales, M. A. Albiter and F. Zaera, *Nat. Mater.*, 2009, **8**, 132.
- 23 I. Lee and F. Zaera, *J. Catal.*, 2010, **269**, 359.
- 24 I. Lee and F. Zaera, *Top. Catal.*, 2013, **56**, 1284.
- 25 P. Gallezot and D. Richard, *Catal. Rev. Sci. Technol.*, 1998, **40**, 81.
- 26 P. Mäki-Arvela, J. Hájek, T. Salmi and D. Y. Murzin, *Appl. Catal., A*, 2005, **292**, 1.
- 27 Y. Yuan, S. Yao, M. Wang, S. Lou and N. Yan, *Curr. Org. Chem.*, 2013, **17**, 400.
- 28 W. W. Yu and H. Liu, *J. Mol. Catal. A: Chem.*, 2006, **243**, 120.
- 29 P. G. N. Mertens, H. Poelman, X. Ye, I. F. J. Vankelecom, P. A. Jacobs and D. E. De Vos, *Catal. Today*, 2007, **122**, 352.
- 30 W. O. Oduro, N. Cailuo, K. M. K. Yu, H. Yang and S. C. Tsang, *Phys. Chem. Chem. Phys.*, 2011, **13**, 2590.
- 31 A. Giroir-Fendler, D. Richard and P. Gallezot, *Catal. Lett.*, 1990, **5**, 175.
- 32 W. Koo-amornpattana and J. M. Winterbottom, *Catal. Today*, 2001, **66**, 277.
- 33 M. Lashdaf, J. Lahtinen, M. Lindblad, T. Venäläinen and A. O. I. Krause, *Appl. Catal., A*, 2004, **276**, 129.
- 34 A. J. Plomp, H. Vuori, A. O. I. Krause, K. P. de Jong and J. H. Bitter, *Appl. Catal., A*, 2008, **351**, 9.
- 35 J. C. Serrano-Ruiz, A. López-Cudero, J. Solla-Gullón, A. Sepúlveda-Escribano, A. Aldaz and F. Rodríguez-Reinoso, *J. Catal.*, 2008, **253**, 159.
- 36 E. V. Ramos-Fernández, J. M. Ramos-Fernández, M. Martínez-Escandell, A. Sepúlveda-Escribano and F. Rodríguez-Reinoso, *Catal. Lett.*, 2009, **133**, 267.
- 37 M. S. Ide, B. Hao, M. Neurock and R. J. Davis, *ACS Catal.*, 2012, **2**, 671.
- 38 J. Shi, R. Nie, P. Chen and Z. Hou, *Catal. Commun.*, 2013, **41**, 101.
- 39 L. R. Baker, G. Kennedy, J. Krier, M. Spronsen, R. Onorato and G. Somorjai, *Catal. Lett.*, 2012, **142**, 1286.
- 40 Z. Niu and Y. Li, *Chem. Mater.*, 2013, DOI: 10.1021/cm4022479.
- 41 F. Zaera, *Chem. Soc. Rev.*, 2013, **42**, 2746.
- 42 F. Zaera, *Int. Rev. Phys. Chem.*, 2002, **21**, 433.

- 1 42 F. Zaera, *ChemCatChem*, 2012, 4, 1525.
- 43 H. Tiznado, S. Fuentes and F. Zaera, *Langmuir*, 2004, 20, 10490.
- 44 I. Lee, J. Ge, Q. Zhang, Y. Yin and F. Zaera, *Nano Res.*, 2011, 4, 115.
- 5 45 M. A. Albiter and F. Zaera, *Langmuir*, 2010, 26, 16204.
- 46 J. Li, X. Liang, J. B. Joo, I. Lee, Y. Yin and F. Zaera, *J. Phys. Chem. C*, 2013, 117, 20043.
- 47 P. Hollins, *Surf. Sci. Rep.*, 1992, 16, 51.
- 10 48 N. Sheppard and C. De La Cruz, *Catal. Today*, 2001, 70, 3.
- 49 A. M. Bradshaw and F. M. Hoffmann, *Surf. Sci.*, 1978, 72, 513.
- 50 M. J. Kappers and J. H. van der Maas, *Catal. Lett.*, 1991, 10, 365.
- 15 51 G. Pérez-Osorio, F. Castellón, A. Simakov, H. Tiznado, F. Zaera and S. Fuentes, *Appl. Catal., B*, 2007, 69, 219.
- 52 S. Galvagno, G. Capannelli, G. Neri, A. Donato and R. Pietropaolo, *J. Mol. Catal.*, 1991, 64, 237.
- 53 G. Szöllösi, B. Török, G. Szakonyi, I. Kun and M. Bartók, *Appl. Catal., A*, 1998, 172, 225.
- 54 M. Arai, K.-I. Usui and Y. Nishiyama, *J. Chem. Soc., Chem. Commun.*, 1993, 1853.
- 55 P. Beccat, J. C. Bertolini, Y. Gauthier, J. Massardier and P. Ruiz, *J. Catal.*, 1990, 126, 451.
- 56 J. C. de Jesús and F. Zaera, *J. Mol. Catal. A: Chem.*, 1999, 138, 237.
- 10 57 J. C. de Jesús and F. Zaera, *Surf. Sci.*, 1999, 430, 99.
- 58 F. Delbecq and P. Sautet, *J. Catal.*, 2002, 211, 398.
- 59 D. Loffreda, F. Delbecq, F. Vigne and P. Sautet, *Angew. Chem., Int. Ed.*, 2005, 44, 5279.
- 60 D. Loffreda, F. Delbecq, F. Vigne and P. Sautet, *J. Am. Chem. Soc.*, 2006, 128, 1316.

20

20

25

25

30

30

35

35

40

40

45

45

50

50

55

55